Black hole subregion action and complexity

Mohsen Alishahiha,[1,*] Komeil Babaei Velni,[2,†] and M. Reza Mohammadi Mozaffar[2,1,‡]
[1]*School of Physics, Institute for Research in Fundamental Sciences (IPM), P.O. Box 19395-5531, Tehran, Iran*
[2]*Department of Physics, University of Guilan, P.O. Box 41335-1914, Rasht, Iran*

(Received 24 February 2019; published 25 June 2019)

We evaluate finite part of the on-shell action for black brane solutions of Einstein gravity on different subregions of spacetime enclosed by null boundaries. These subregions include the intersection of the Wheeler-DeWitt patch with past/future interior and left/right exterior for a two-sided black brane. Identifying the on-shell action on the exterior regions with subregion complexity, one finds that it obeys the subadditivity condition. This gives an insight to define a new quantity named mutual complexity. We will also consider a certain subregion that is a part of spacetime, which could be causally connected to an operator localized behind/outside the horizon. Taking into account all terms needed to have a diffeomorphism-invariant action with a well-defined variational principle, one observes that the main contribution that results in a nontrivial behavior of the on-shell action comes from joint points where two lightlike boundaries (including the horizon) intersect. A spacelike boundary gives rise to a linear time growth, while we have a classical contribution due to a timelike boundary that is given by the free energy.

DOI: 10.1103/PhysRevD.99.126016

I. INTRODUCTION

Based on the earlier works of Refs. [1,2], it was conjectured that computational complexity associated with a boundary state may be identified with the on-shell action evaluated on a certain subregion of the bulk spacetime [3,4]. The corresponding subregion is Wheeler-DeWitt (WDW) patch of the spacetime that is the domain of dependence of any Cauchy surface in the bulk of which the intersection with the asymptotic boundary is the time slice on which the state is defined.

This proposal, known as "complexity equals action" (CA), has been used to explore several properties of computational complexity for those field theories that have a gravitational dual.[1] In particular, the growth rate of complexity has been studied for an eternal black hole in Ref. [18]. It was shown that, although in the late time the growth rate approaches a constant value that is twice the mass of the black hole, the constant is approached from above, violating the Lloyd's bound [19]. Of course, this is not the case for a state followed by a global quench [20]. It is worth mentioning that recently there has been some progress for studying the computational complexity of a state in field theory[21–32].

So far, the main concern in the literature was the growth rate of complexity, and therefore the on-shell action was computed up to time-independent terms [33–35]. Moreover, it was also shown that the time-dependent effects are controlled by the regions behind the horizon. We note, however, that in order to understand holographic complexity better it is crucial to have the full expression of it. It is also important to evaluate the contribution of different parts (inside and outside of the horizon) of the WDW patch, especially. It is also illustrative to compute the on-shell action on a given subregion of spacetime enclosed by null boundaries, which is not necessarily the WDW patch. Indeed, one of the aims of the present work is to carry out these computations explicitly. Moreover, we will carefully identify the contribution of each term in the action.

Since we are interested in the on-shell action, it is crucial to make clear what one means by "on-shell action." In general, an action could have several terms that might be important due to a certain physical reason. In particular, in order to have a well-defined variational principle with the

*alishah@ipm.ir
†babaeivelni@guilan.ac.ir
‡mmohammadi@guilan.ac.ir

[1]We would like to stress that on the gravity side there is another proposal for computing the computational complexity, known as "complexity equals volume" (CV) [1,2]. The generalization of the CV proposal to subsystems has been done in Ref. [5] (see also Refs. [6–13]). Yet another approach to complexity based on Euclidean path integral has been introduced in Refs. [14–16]. For a recent development and its possible relation to the CA approach, see Ref. [17].

Dirichlet boundary condition, one needs to add certain Gibbons-Hawking-York boundary terms at spacelike and timelike boundaries [36,37]. Moreover, to accommodate null boundaries, it is also crucial to add the corresponding boundary terms on the null boundaries as well as certain joint action at points where a null boundary intersects other boundaries [38,39].

Restricted to Einstein gravity and assuming to have a well-defined variational principle, one arrives at the following action [39]:

$$I^{(0)} = \frac{1}{16\pi G_N}\int d^{d+2}x\sqrt{-g}(R-2\Lambda) + \frac{1}{8\pi G_N}\int_{\Sigma_t^{d+1}} K_t d\Sigma_t \pm \frac{1}{8\pi G_N}\int_{\Sigma_s^{d+1}} K_s d\Sigma_s \pm \frac{1}{8\pi G_N}\int_{\Sigma_n^{d+1}} K_n dS d\lambda \pm \frac{1}{8\pi G_N}\int_{J^d} a dS. \tag{1.1}$$

Here, the timelike, spacelike, and null boundaries and also joint points are denoted by $\Sigma_t^{d+1}, \Sigma_s^{d+1}, \Sigma_n^{d+1}$, and J^d, respectively. The extrinsic curvature of the corresponding boundaries are given by K_t, K_s, and K_n. The function a at the intersection of the boundaries is given by the logarithm of the inner product of the corresponding normal vectors, and λ is the null coordinate defined on the null segments. The sign of different terms depends on the relative position of the boundaries and the bulk region of interest (see Ref. [39] for more details).

As far as the variational principle is concerned, the above action defines a consistent theory. Nonetheless, one still has possibilities to add certain boundary terms that do not alter the boundary condition but could have a nontrivial contribution to the on-shell action. Therefore, it is important to fix these terms using certain physical principles before computing the on-shell action.

In particular, one can see that the above action is not invariant under a reparametrization of the null generators. Therefore, one may conclude that the above action does not really define a consistent theory. Actually, to maintain the invariance under a reparametrization of the null generators, one needs to add an extra term to the action as [39] (see also Ref. [40])[2]

$$I^{\rm amb} = \frac{1}{8\pi G_N}\int_{\Sigma_n^{d+1}} d^d x d\lambda\sqrt{\gamma}\Theta\log\frac{|\tilde{L}\Theta|}{d}, \tag{1.2}$$

where $\tilde{L}$ is an undetermined length scale and γ is the determinant of the induced metric on the joint point where two null segments intersect, and

$$\Theta = \frac{1}{\sqrt{\gamma}}\frac{\partial\sqrt{\gamma}}{\partial\lambda}. \tag{1.3}$$

Although even with this extra term the length scale $\tilde{L}$ remains undetermined, adding this term to action (1.1) would define a consistent theory. Therefore, in what follows, by evaluating on-shell action, we mean to consider $I = I^{(0)} + I^{\rm amb}$. We note, however, that the resultant on-shell action may or may not be UV finite. Thus, one may want to get the finite on-shell action (as we do for gravitational free energy) that requires adding certain counterterms. Actually, these terms are also required from holographic renormalization (see, e.g., Ref. [44]). Of course, in this paper, we will not consider such counterterms nor those needed due to null boundaries [45].

The aim of this article is to compute on-shell action on certain subregions behind and outside the horizon enclosed by null boundaries. We will consider an eternal black brane that provides a gravitational dual for a thermofield double state. Those subregions that are behind the horizon are UV finite and time dependent, though those outside the horizon are typically UV divergent and time independent.

To proceed, we will consider a $(d+2)$-dimensional black brane solution in Einstein gravity of which the metric is[3]

$$ds^2 = \frac{L^2}{r^2}\left(-f(r)dt^2 + \frac{dr^2}{f(r)} + \sum_{i=1}^{d} d\vec{x}^2\right),$$
$$f(r) = 1 - \left(\frac{r}{r_h}\right)^{d+1}, \tag{1.4}$$

where r_h is the radius of horizon and L denotes the anti-de Sitter (AdS) radius. In terms of these parameters, the entropy, mass, and Hawking temperature of the corresponding black brane are

$$S_{th} = \frac{V_d L^d}{4G_N r_h^d}, \quad M = \frac{V_d L^d}{16\pi G_N}\frac{d}{r_h^{d+1}}, \quad T = \frac{d+1}{4\pi r_h}, \tag{1.5}$$

with V_d being the volume of d-dimensional internal space of the metric parametrized by x_i, $i = 1, \cdots d$. It is also useful to note that

$$\sqrt{-g}(R-2\Lambda) = -2(d+1)\frac{L^d}{r^{d+2}}. \tag{1.6}$$

The organization of the paper is as follows. In the next section, we will consider on-shell action on the WDW patch which according to CA proposal may be related to the holographic complexity of the dual state. Our main concern is to present a closed form for the on-shell action. We will

[2]The importance of this term has also been emphasized in Refs. [41–43], in which it was shown that it is essential to consider the contribution of this term to the complexity.

[3]Because of the flat boundary of the black brane solution, we will be able to present our results in simple compact forms.

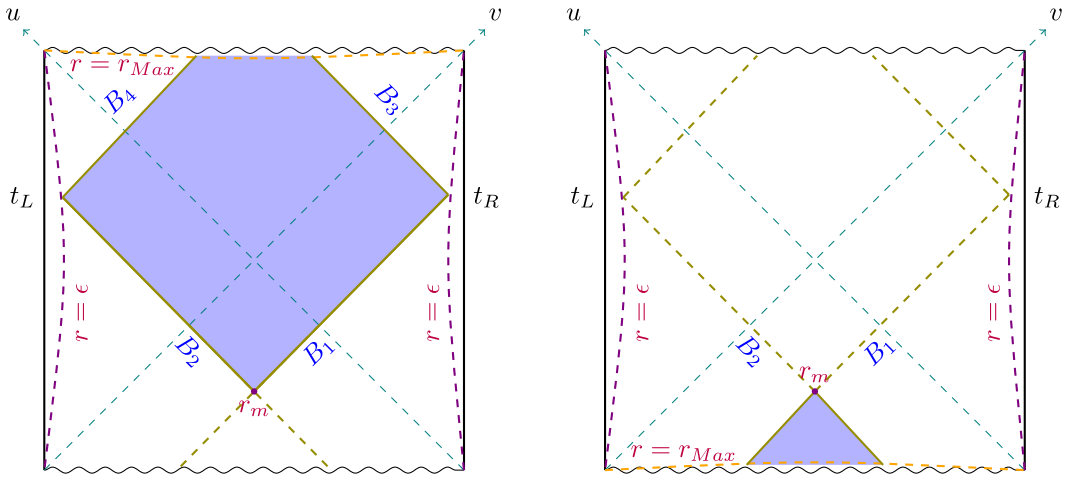

FIG. 1. Penrose diagram of the WDW patch of an eternal AdS black hole assuming $t_R = t_L$. *Left*: WDW patch on which the on-shell action is computed to find the complexity. *Right*: Past patch corresponding to the WDW patch. The past patch may be identified as a part that is casually connected to an operator localized at $r = r_m$ behind the horizon.

also compute the on-shell action for a past patch that is obtained by continuing the past null boundaries all the way to the past singularity. We will also compute on-shell action on the intersection of the WDW patch with past and future interiors. We study the time evolution of holographic uncomplexity, too. In Sec. III, we will consider different patches that are outside the horizon. This includes the intersection of the WDW patch with the entanglement wedge that could be thought of as CA subregion complexity. The last section is devoted to a discussion and conclusion, in which we present the interpretation of our results.

II. COMPLEXITY AND SUBREGIONS BEHIND THE HORIZON

A. CA proposal

In this section, using CA proposal, we would like to evaluate complexity for the eternal two-sided black brane, which is dual to the thermofield double state in the boundary theory. Holographically, one should compute on-shell action on the WDW patch as depicted in the left panel of Fig. 1. Using the symmetry of the Penrose diagram of the eternal black hole, we shall consider a symmetric configuration with times $t_R = t_L = \frac{\tau}{2}$. Actually, this question has already been addressed [18]; the full time dependence of complexity has been obtained, and it was shown that the holographic complexity violates the Lloyd bound in this case.[4] Of course, our main interest in the present paper is to study the finite part of the on-shell action. In this subsection, we will present the results and computations rather in details. Because of the similarity of computations, in the rest of the paper, the computations will be a little bit brief.

To proceed, we note that the null boundaries of the corresponding WDW patch are (see the left panel of Fig. 1)

$$B_1: t = t_R - r^*(\epsilon) + r^*(r), \quad B_2: t = -t_L + r^*(\epsilon) - r^*(r),$$
$$B_3: t = t_R + r^*(\epsilon) - r^*(r), \quad B_4: t = -t_L - r^*(\epsilon) + r^*(r), \tag{2.1}$$

and the position of the joint point r_m is given by[5]

$$\tau \equiv t_L + t_R = 2(r^*(\epsilon) - r^*(r_m)). \tag{2.2}$$

Let us now compute the on-shell action over the corresponding WDW patch. As we already mentioned, the action consists of several parts that include the bulk, boundaries, and joint actions. Using Eq. (1.6), the bulk action is [18]

$$I^{\text{bulk}}_{\text{WDW}} = -\frac{V_d L^d}{4\pi G_N}(d+1)\left(2\int_\epsilon^{r_{\text{Max}}} \frac{dr}{r^{d+2}}(r^*(\epsilon) - r^*(r)) + \int_{r_m}^{r_{\text{Max}}} \frac{dr}{r^{d+2}}\left(\frac{\tau}{2} - r^*(\epsilon) + r^*(r)\right)\right). \tag{2.3}$$

By making use of an integration by parts, the above bulk action reads

$$I^{\text{bulk}}_{\text{WDW}} = -\frac{V_d L^d}{4\pi G_N}\left(2\int_\epsilon^{r_{\text{Max}}} \frac{dr}{r^{d+1}f(r)} - \int_{r_m}^{r_{\text{Max}}} \frac{dr}{r^{d+1}f(r)}\right) = -\frac{V_d L^d}{4\pi G_N}\left(\frac{\tau+\tau_c}{2r_h^{d+1}} + \frac{2}{d\epsilon^d} - \frac{1}{dr_m^d}\right), \tag{2.4}$$

[4]The one-sided black hole was also discussed in Refs. [20,41–43], in which it was confirmed that in this case the Lloyd bound is respected.

[5]Note that in our notation one has $r^*(r) \leq 0$.

where $\tau_c = 2(r^*(\epsilon) - r^*(r_{Max}))$ is the critical time below which the time derivative of complexity vanishes [4,18]. More explicitly, one has (see also Ref. [18])

$$\tau_c = \frac{1}{2T}\frac{1}{\sin\frac{\pi}{d+1}}. \tag{2.5}$$

To find the boundary contributions, we note that using the affine parametrization for the null directions the corresponding boundary terms vanish[6] and we are left with just a spacelike boundary at future singularity of which the contribution is given by

$$I^{\rm surf}_{\rm WDW} = -\frac{1}{8\pi G_N}\int d^dx \int_{-t_L - r^*(\epsilon)+r^*(r)}^{t_R + r^*(\epsilon)-r^*(r)} dt\sqrt{h}K_s|_{r=r_{\rm Max}}, \tag{2.6}$$

where K_s is the trace of extrinsic curvature of the boundary at $r = r_{\rm Max}$ and h is the determinant of the induced metric. To compute this term, it is useful to note that for a constant r surface using the metric (1.4) one has

$$\sqrt{h}K = -\sqrt{g^{rr}}\partial_r\sqrt{h} = -\frac{1}{2}\frac{L^d}{r^d}\left(\partial_r f(r) - \frac{2(d+1)}{r}f(r)\right). \tag{2.7}$$

Plugging the above expression into (2.6) and evaluating it at $r = r_{\rm Max}$, one finds

$$I^{\rm surf}_{\rm WDW} = \frac{V_d L^d}{8\pi G_N}(d+1)\frac{\tau+\tau_c}{2r_h^{d+1}}. \tag{2.8}$$

There are also several joint points that may contribute to the on-shell action. Two of them are located at the future singularity that has zero contributions, while the contributions of the three remaining points at $r = \epsilon$ and $r = r_m$ are given by

$$I^{\rm joint}_{\rm WDW} = 2\times\frac{-1}{8\pi G_N}\int_\epsilon d^dx\sqrt{\gamma}\log\frac{|k_1\cdot k_2|}{2} + \frac{1}{8\pi G_N}\int_{r_m} d^dx\sqrt{\gamma}\log\frac{|k_1\cdot k_2|}{2}, \tag{2.9}$$

where the factor of 2 is due to the two joint points at $r = \epsilon$ for left and right boundaries. Here, k_1 and k_2 are the null vectors associated with the null boundaries

$$k_1 = \alpha\left(-dt + \frac{dr}{f(r)}\right), \qquad k_2 = \beta\left(dt + \frac{dr}{f(r)}\right). \tag{2.10}$$

Here, α and β are two constants appearing due to the ambiguity of the normalization of normal vectors of null segments. Therefore, one gets

$$I^{\rm joint}_{\rm WDW} = -\frac{V_d L^d}{4\pi G_N}\frac{\log\frac{\alpha\beta\epsilon^2}{L^2}}{\epsilon^d} + \frac{V_d L^d}{8\pi G_N}\left(\frac{\log\frac{\alpha\beta r_m^2}{L^2}}{r_m^d} - \frac{\log|f(r_m)|}{r_m^d}\right). \tag{2.11}$$

It is clear from the above expression that the result suffers from an ambiguity associated with the normalization of null vectors. This ambiguity may be fixed either by fixing the constants α and β by hand or adding a proper term to the action. Actually, as we have already mentioned, in order to maintain the diffeomorphism invariance of the action, we will have to add another term given by Eq. (1.2). Note that, even with this term, we are still left with an undetermined free parameter. In the present case, taking into account all four null boundaries, one gets[7]

$$I^{\rm amb}_{\rm WDW} = -\frac{V_d L^d}{8\pi G_N}\left(\frac{\log\frac{\alpha\beta\tilde{L}^2 r_m^2}{L^4}}{r_m^d} + \frac{2}{dr_m^d}\right) + \frac{V_d L^d}{4\pi G_N}\left(\frac{\log\frac{\alpha\beta\tilde{L}^2\epsilon^2}{L^4}}{\epsilon^d} + \frac{2}{d\epsilon^d}\right). \tag{2.12}$$

Now, we have all terms in the action evaluated on the WDW patch. Therefore, one arrives at

$$I_{\rm WDW} = I^{\rm bulk} + I^{\rm surf} + I^{\rm joint} + I^{\rm amb} = \frac{V_d L^d}{8\pi G_N}\left[\frac{2}{\epsilon^d}\log\frac{\tilde{L}^2}{L^2} + \frac{d-1}{2r_h^{d+1}}(\tau+\tau_c) - \frac{\log\frac{\tilde{L}^2|f(r_m)|}{L^2}}{r_m^d}\right]. \tag{2.13}$$

It is important to note that in order to have a meaningful result the divergent term should be positive, which is the case for $\tilde{L} \geq L$. On the other hand, setting $\tilde{L} = L$, the divergent term will drop, and one gets a finite result consisting of two contributions[8]: one from the future

[6]For affine parametrization of the null direction, the extrinsic curvature of the null boundary will be zero, and therefore there is no contribution from null boundaries. In this paper, we always use this parametrization, and therefore we do not need to consider the boundary terms for null boundaries.

[7]Note that for the boundary associated with k_1 one has $\frac{dr}{d\lambda} = \alpha\frac{r^2}{L^2}$ and $\Theta = 2d\alpha\frac{r}{L^2}$. For the other null vector, one should replace α with β.

[8]Actually, in the context of holographic renormalization, one would add certain counterterms to make the on-shell action finite. In the present case, to remove the divergent term, one may add a counterterm in the form

$$I^{\rm ct} = \frac{1}{8\pi G_N}\int d\lambda d^dx\sqrt{\gamma}\Theta\log\frac{L^2}{\tilde{L}^2},$$

which is essentially equivalent to setting $\tilde{L} = L$, and then we are left with the finite on-shell action. Of course, in this paper, we keep the length scale $\tilde{L}$ undetermined.

spacelike singularity and a contribution from the joint point at $r = r_m$ given as

$$I_{\rm WDW} = \frac{V_d L^d}{8\pi G_N}\left[\frac{d-1}{2r_h^{d+1}}(\tau+\tau_c) - \frac{\log|f(r_m)|}{r_m^d}\right]. \quad (2.14)$$

It is also interesting to note that for $r_m \to r_{\rm Max}$ where $\tau \to \tau_c$, one gets

$$I_{\rm WDW} = \frac{V_d L^d}{8\pi G_N}\frac{d-1}{r_h^{d+1}}\tau_c = \frac{d-1}{d+1}\frac{S_{th}}{\sin\frac{\pi}{d-1}}, \quad (2.15)$$

which is identically zero for $d = 1$. This might be thought of as complexity of formation of the black brane [46]. On the other hand, using the fact that $\log|f(r_m)| \approx -\frac{(d+1)\tau}{2r_h}$ for $r_m \to r_h$ (see the next section), one gets the linear growth at late times,

$$I_{\rm WDW} \approx \frac{V_d L^d}{8\pi G_N}\frac{d}{r_h^{d+1}}\tau = 2M\tau, \quad (2.16)$$

as expected.

B. Past patch

In this subsection, we would like to compute the on-shell action on the past patch defined by the colored triangle shown in the right panel of Fig. 1. Clearly, the rate of change of the on-shell action on the past patch is the same as that of the WDW patch. Another way to think of the past patch is to consider an operator localized at $r = r_m$ behind the horizon. The part of spacetime that can be causally connected to the operator is the triangle depicted in Fig. 1. Following the CA proposal, one may think of the on-shell action evaluated on the past patch as the complexity associated with the operator.

Let us compute the on-shell action for the past patch. To proceed, we note that, using the notation of the previous subsection, the contribution of the bulk term to the on-shell action is

$$\begin{aligned} I^{\rm bulk}_{\rm past} &= -\frac{V_d L^d}{8\pi G_N}(d+1)\int_{r_m}^{r_{\rm Max}}\frac{dr}{r^{d+2}}\int_{-t_L+r^*(0)-r^*(r)}^{t_R-r^*(0)+r^*(r)} dt \\ &= \frac{V_d L^d}{4\pi G_N}\int_{r_m}^{r_{\rm Max}}\frac{dr}{r^{d+1}f} = \frac{V_d L^d}{4\pi G_N}\left(\frac{\tau-\tau_c}{2r_h^{d+1}} + \frac{1}{dr_m^d}\right). \end{aligned} \quad (2.17)$$

Here, to get the second line, we have performed an integration by parts. On the other hand, the contribution of the spacelike boundary at past singularity is found to be

$$\begin{aligned} I^{\rm surf}_{\rm past} &= \frac{1}{8\pi G_N}\int d^d x\int_{-t_L+r^*(0)-r^*(r)}^{t_R-r^*(0)+r^*(r)} dt\sqrt{h}K_s|_{r=r_{\rm Max}} \\ &= \frac{V_d L^d}{8\pi G_N}(d+1)\frac{\tau-\tau_c}{2r_h^{d+1}}. \end{aligned} \quad (2.18)$$

There are also three joint points, two of which are at $r = r_{\rm Max}$ and one of which is at $r = r_m$. The corresponding contributions to the on-shell action for those at $r_{\rm Max}$ vanish for large $r_{\rm Max}$, while the contribution of that at $r = r_m$ is given by

$$\begin{aligned} I^{\rm joint}_{\rm past} &= \frac{1}{8\pi G_N}\int d^{d-1}x\sqrt{\gamma}\log\frac{|k_1\cdot k_2|}{2} \\ &= \frac{V_d L^d}{8\pi G_N}\left(\frac{\log\frac{\alpha\beta r_m^2}{L^2}}{r_m^d} - \frac{\log|f(r_m)|}{r_m^d}\right). \end{aligned} \quad (2.19)$$

Finally, the contribution of the term needed to remove the ambiguity is

$$I^{\rm amb}_{\rm past} = -\frac{V_d L^d}{8\pi G_N}\left(\frac{\log\frac{\alpha\beta\tilde{L}^2 r_m^2}{L^4}}{r_m^d} + \frac{2}{dr_m^d}\right). \quad (2.20)$$

Therefore, altogether one arrives at

$$I_{\rm past} = \frac{V_d L^d}{8\pi G_N}\left(\frac{d-1}{2r_h^{d+1}}(\tau-\tau_c) - \frac{\log\frac{\tilde{L}^2|f(r_m)|}{L^2}}{r_m^d}\right), \quad (2.21)$$

which is UV finite even with arbitrary finite length scale $\tilde{L}$. Note that for $r_m \to r_{\rm Max}$ where $\tau \to \tau_c$ the on-shell action for the past patch vanishes identically. On the other hand, in the late times when $r_m \to r_h$, one finds linear growth as expected.

C. Intersection of WDW patch with past and future interiors

Even for a static geometry, such as an eternal black hole, the interior of black hole grows with time, indicating that there could be a quantity in the dual field theory that grows with time far after the system reaches the thermal equilibrium. Indeed, this was the original motivation for holographic computational complexity to be identified with the volume of the black hole interior.

In the previous subsection, we computed the on-shell action over the whole WDW patch. The aim of this subsection is to compute on-shell action in the intersection of the WDW patch with the black brane interior. This consists of past and future interiors as shown in Fig. 2. Actually, these subregions are the main parts that contribute to the time dependence of the complexity of the dual state. It is, however, instructive to study these parts separately.[9]

[9]The on-shell action for the subregion in the black hole interior has also been studied in Ref. [47], where it was argued that complexity may be used as a probe to study the nature of different singularities.

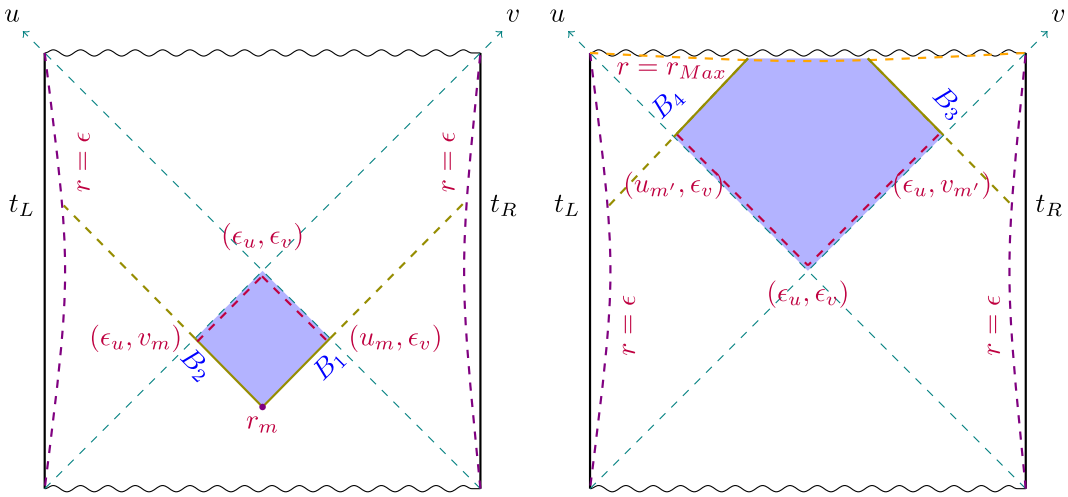

FIG. 2. *Left:* Intersection of the WDW patch with the past interior. *Right:* Intersection of the WDW patch with the future interior.

1. Past interior

To begin with, we first consider the intersection of the WDW patch with the past interior as shown in the left panel of Fig. 2. Actually, one may use the results of the previous subsection to write different terms contributing to the on-shell action. To start with, we note that for the bulk term one has

$$I_{\rm PI}^{\rm bulk}=\frac{V_dL^d}{4\pi G_N}(d+1)\int_{r_h}^{r_m}\frac{dr}{r^{d+2}}\left(\frac{\tau}{2}-r^*(\epsilon)+r^*(r)\right)$$
$$=\frac{V_dL^d}{4\pi G_N}\left(\frac{1}{dr_m^d}-\frac{1}{dr_h^d}\right). \tag{2.22}$$

There are four joint points, one at $r=r_m$ and three at $r=r_h$, that contribute to the on-shell action. It is, however, important to note that those points at the horizon are not at the same point. In other words, the radial coordinate r is not suitable for making a distinction between these points. Indeed, to distinguish between these points, following Ref. [48], it is convenient to use the following coordinate system for the past interior:

$$u=-e^{-\frac{1}{2}f'(r_h)(r^*(r)-t)},\qquad v=-e^{-\frac{1}{2}f'(r_h)(r^*(r)+t)}. \tag{2.23}$$

In this coordinate system, the horizon is located at $uv=0$ [i.e., $r^*(r_h)=-\infty$]. This equation has three nontrivial solutions given by $(u=0,v\neq 0)$, $(u\neq 0,v=0)$, and $(u=0,v=0)$ that correspond to three joint points at the horizon shown in Fig. 2. Since both $r^*(r)$ and $\log f(r)$ are singular at $r=r_h$, one may regularize the contribution of these three points by setting the horizon at $v=\epsilon_v$ and $u=\epsilon_u$. In this notation, the joint points are given by (ϵ_u,v_m), (u_m,ϵ_v), and (ϵ_u,ϵ_v) as depicted in Fig. 2. In what follows, the radial coordinates associated with these three points are denoted by r_{v_m}, r_{u_m} and r_ϵ, respectively. Using this notation, the contribution of joint points is

$$I_{\rm PI}^{\rm joint}=\frac{V_dL^d}{8\pi G_N}\left(\frac{\log\frac{\alpha\beta r_m^2}{L^2|f(r_m)|}}{r_m^d}-\frac{\log\frac{\alpha\beta r_{u_m}^2}{L^2|f(r_{u_m})|}}{r_{u_m}^d}-\frac{\log\frac{\alpha\beta r_{v_m}^2}{L^2|f(r_{v_m})|}}{r_{v_m}^d}+\frac{\log\frac{\alpha\beta r_\epsilon^2}{L^2|f(r_\epsilon)|}}{r_\epsilon^d}\right)$$
$$=-\frac{V_dL^d}{8\pi G_N}\left(\frac{\log|f(r_m)|}{r_m^d}+\frac{\log|f(r_\epsilon)|-\log|f(r_{u_m})|-\log|f(r_{v_m})|}{r_h^d}+\frac{\log\frac{\alpha\beta r_h^2}{L^2}}{r_h^d}-\frac{\log\frac{\alpha\beta r_m^2}{L^2|}}{r_m^d}\right). \tag{2.24}$$

Here, we have used the fact that $\{r_{u_m},r_{v_m},r_\epsilon\}\approx r_h$. On the other hand, by making use of the fact that [48]

$$\log|f(r_{u,v})|=\log|uv|+c_0+\mathcal{O}(uv)\quad\text{for } uv\to 0, \tag{2.25}$$

one gets

$$\log|f(r_{u_m})|=\log|u_m\epsilon_v|+c_0+\mathcal{O}(\epsilon_v),$$
$$\log|f(r_{v_m})|=\log|\epsilon_u v_m|+c_0+\mathcal{O}(\epsilon_u),$$
$$\log|f(r_\epsilon)|=\log|\epsilon_u\epsilon_v|+c_0+\mathcal{O}(\epsilon_u\epsilon_v), \tag{2.26}$$

which can be used to simplify (2.24) as follows:

$$I_{\rm PI}^{\rm joint}=-\frac{V_dL^d}{8\pi G_N}\left(\frac{\log|f(r_m)|}{r_m^d}-\frac{\log(u_mv_m)+c_0}{r_h^d}+\frac{\log\frac{\alpha\beta r_h^2}{L^2}}{r_h^d}-\frac{\log\frac{\alpha\beta r_m^2}{L^2}}{r_m^d}\right). \tag{2.27}$$

Here, $c_0=\psi^{(0)}(1)-\psi^{(0)}(\frac{1}{d+1})$ is a positive number, and $\psi^{(0)}(x)=\frac{\Gamma'(x)}{\Gamma(x)}$ is the digamma function.

Finally, one has to remove the ambiguity due to the normalization of the null vectors by adding the extra term (1.2) to the action. The resulting expression is then

$$I_{\rm PI}^{\rm amb}=-\frac{V_dL^d}{8\pi G_N}\left(\frac{\log\frac{\alpha\beta\tilde{L}^2r_m^2}{L^4}}{r_m^d}+\frac{2}{dr_m^d}\right)+\frac{V_dL^d}{8\pi G_N}\left(\frac{\log\frac{\alpha\beta\tilde{L}^2r_h^2}{L^4}}{r_h^d}+\frac{2}{dr_h^d}\right). \tag{2.28}$$

Therefore, altogether for the subregion given by the intersection of the WDW patch with the past interior shown in the left panel of Fig. 2, one gets

$$I_{\rm PI}=\frac{V_dL^d}{8\pi G_N}\left(\frac{1}{r_h^d}\log\frac{\tilde{L}^2}{L^2}+\frac{c_0}{r_h^d}-\frac{(d+1)\tau}{2r_h^{d+1}}-\frac{\log\frac{\tilde{L}^2|f(r_m)|}{L^2}}{r_m^d}\right), \tag{2.29}$$

which depends on time through its r_m dependence, as expected. Here, we have used the fact that $\log(u_mv_m)=-f'(r_h)r^*(r_m)=-\frac{(d+1)\tau}{2r_h}$. Note that for $r_m\to r_{\rm Max}$ the time dependence of the on-shell action drops out, resulting in

$$I_{\rm PI}=\left(c_0-\frac{(d+1)\tau_c}{2r_h}+\log\frac{\tilde{L}^2}{L^2}\right)\frac{S_{th}}{2\pi}. \tag{2.30}$$

Note also that at late times when $r_m\to r_h$, using Eq. (2.25), the total on-shell action in the past interior vanishes.

2. Future interior

Let us now compute on-shell action for the intersection of the WDW patch with the future interior shown in the right panel of Fig. 2. In this case, using our previous results, the bulk term of the action is

$$I_{\rm FI}^{\rm bulk}=-\frac{V_dL^d}{4\pi G_N}(d+1)\int_{r_h}^{r_{\rm Max}}\frac{dr}{r^{d+2}}\left(\frac{\tau}{2}+r^*(\epsilon)-r^*(r)\right)=-\frac{V_dL^d}{4\pi G_N}\left(\frac{1}{dr_h^d}+\frac{\tau+\tau_c}{2r_h^{d+1}}\right). \tag{2.31}$$

There are five joint points, two of which have zero contributions for large $r_{\rm Max}$, while the contributions of other three points are given by

$$\begin{aligned}I_{\rm FI}^{\rm joint}&=\frac{V_dL^d}{8\pi G_N}\left(\frac{\log\frac{\alpha\beta r_\epsilon^2}{L^2|f(r_\epsilon)|}}{r_\epsilon^d}-\frac{\log\frac{\alpha\beta r_{u_{m'}}^2}{L^2|f(r_{u_{m'}})|}}{r_{u_{m'}}^d}-\frac{\log\frac{\alpha\beta r_{v_{m'}}^2}{L^2|f(r_{v_{m'}})|}}{r_{v_{m'}}^d}\right)\\&=-\frac{V_dL^d}{8\pi G_N}\left(\frac{\log|f(r_\epsilon)|-\log|f(r_{u_{m'}})|-\log|f(r_{v_{m'}})|}{r_h^d}+\frac{\log\frac{\alpha\beta r_h^2}{L^2}}{r_h^d}\right)\\&=\frac{V_dL^d}{8\pi G_N}\left(\frac{\log|u_{m'}v_{m'}|+c_0}{r_h^d}-\frac{\log\frac{\alpha\beta r_h^2}{L^2}}{r_h^d}\right).\end{aligned} \tag{2.32}$$

The boundary terms associated with the null boundaries vanish using affine parametrization for the null directions, and the only term we need to compute is the surface term at future singularity. This is indeed the term we have already computed in Eq. (2.8)

$$I_{\rm FI}^{\rm surf}=\frac{V_dL^d}{8\pi G_N}(d+1)\frac{\tau+\tau_c}{2r_h^{d+1}}. \tag{2.33}$$

The only remaining contribution to be computed is the term needed to remove the ambiguity

$$I_{\rm FI}^{\rm amb}=\frac{V_dL^d}{8\pi G_N}\left(\frac{\log\frac{\alpha\beta\tilde{L}^2r_h^2}{L^4}}{r_h^d}+\frac{2}{dr_h^d}\right). \tag{2.34}$$

Taking all terms into account, we have

$$I_{\rm FI}=\frac{V_dL^d}{8\pi G_N}\left(\frac{d\tau}{r_h^{d+1}}+\frac{(d-1)\tau_c}{2r_h^{d+1}}+\frac{c_0}{r_h^d}+\frac{1}{r_h^d}\log\frac{\tilde{L}^2}{L^2}\right). \tag{2.35}$$

Here, to get the final result, we have used the fact that $\log|u_{m'}v_{m'}| = \frac{(d+1)\tau}{2r_h}$.

It is also interesting to sum the contributions of both regions shown in Fig. 2 and compare the resultant expression with the on-shell action evaluated on the whole WDW patch

$$I_{\rm Ext} = I_{\rm WDW} - (I_{\rm PI} + I_{\rm FI}) = 2\times\frac{V_d L^d}{8\pi G_N}\left[-\frac{c_0}{r_h^d} + \left(\frac{1}{\epsilon^d} - \frac{1}{r_h^d}\right)\log\frac{\tilde{L}^2}{L^2}\right], \quad (2.36)$$

which is time independent, as expected. In fact, this is the contribution of the part of the WDW patch that is outside of the black hole horizon. The factor of 2 is a symmetric factor between the left and right sides of the corresponding WDW patch. It is also interesting to note that the finite term is negative. We will consider the above result in the next section, in which we will study subregion complexity.

D. Late-time behavior

In this section, we will study the time derivative of the on-shell actions we have found in the previous subsections. To proceed, we note that from definitions of r^* and r_m one has

$$\frac{dr^*(r_m)}{d\tau} = -\frac{1}{2}, \qquad \frac{dr_m}{d\tau} = \frac{1}{2}f(r_m), \quad (2.37)$$

which can be used to show

$$\frac{dI_{\rm WDW}}{d\tau} = \frac{dI_{\rm past}}{d\tau} = 2M\left(1 + \frac{1}{2}\tilde{f}(r_m)\log\frac{\tilde{L}^2|f(r_m)|}{L^2}\right), \qquad \tilde{f} = \frac{r_h^{d+1}}{r_m^{d+1}} - 1. \quad (2.38)$$

It is also interesting to compute the time derivative of the on-shell action for the individual subregions we have considered before. Actually, it is straightforward to see

$$\frac{dI_{\rm PI}}{d\tau} = M\tilde{f}(r_m)\log\frac{\tilde{L}^2|f(r_m)|}{L^2}, \quad \frac{dI_{\rm FI}}{d\tau} = 2M, \quad \frac{dI_{\rm Ext}}{d\tau} = 0. \quad (2.39)$$

It is evident that summing up these contributions one gets (2.38), as expected. Note that at late times when $r_m \to r_h$ the past interior has no contribution to the rate of complexity growth.

Of course, it is known that the complexity obtained from the WDW patch violates the Lloyd bound, though at late time, it approaches $2M$. From the above results, it is evident that the contribution to the late-time behavior comes from the future interior of the black brane. It is also worth noting that the violation of the Lloyd bound is due to the contribution of the joint point located at the past interior. This, in turn, suggests that if one defines the complexity as on-shell action evaluated on the intersection of the WDW patch and future interior, the resultant complexity fulfills the Lloyd bound and has linear growth at the late time. Of course, if one wants appropriate UV divergences before regularizing the complexity, we should also add the contributions of the exterior region. More explicitly, one has

$$\tilde{I}_{\rm WDW} = I_{FI} + I_{\rm Ext} = 2M\left(\tau + \frac{(d-1)\tau_c - 2c_0 r_h}{d} + \left(\frac{2r_h^{d+1}}{d\epsilon^d} - \frac{r_h}{d}\right)\log\frac{\tilde{L}^2}{L^2}\right). \quad (2.40)$$

It is also instructive to note that at late time when $r_m \to r_h$, setting $r_m - r_h = \xi$, from Eq. (2.2), one finds

$$\tau = -\frac{2r_h}{d+1}\left(\log\frac{(d+1)\xi}{r_h} - c_0\right) \sim \frac{\beta}{2\pi}\log\frac{r_h}{(d+1)\xi}, \quad \text{with} \quad \beta = \frac{1}{T}. \quad (2.41)$$

In particular, when one is away from the horizon about a power of Planck scale $\xi \sim \frac{\ell_p^d}{r_h^{d-1}}$, the above late-time behavior reads

$$\tau \sim \frac{\beta}{2\pi}\log S_{\rm th}, \quad (2.42)$$

in which the on-shell action reads $I \sim S_{\rm th}\log S_{\rm th}$, which is the scrambling complexity. Following Ref. [49], one may also consider the case in which the time is about $\tau \sim \frac{\beta}{2\pi}e^{S_{\rm th}}$, which could be the time when one gets maximum complexity. At that time, the on-shell action is

$$I \sim S_{\rm th}e^{S_{\rm th}}, \quad (2.43)$$

which could be thought of as maximum complexity of the system [49].

E. Holographic uncomplexity

Given a time slice and the associated WDW patch, one may want to compute on-shell action on a region that should be included in the WDW patch as time goes. The corresponding region is shown in Fig. 3. Actually, following Ref. [49], one may identify the on-shell action on this region with "holographic uncomplexity" that is the gap between the complexity and the maximum possible complexity (see also Refs. [50,51]). In other words, the uncomplexity is room for complexity to increase. Alternatively, one could think of the holographic uncomplexity as the spacetime resource available to an observer who intends to enter the horizon [49].

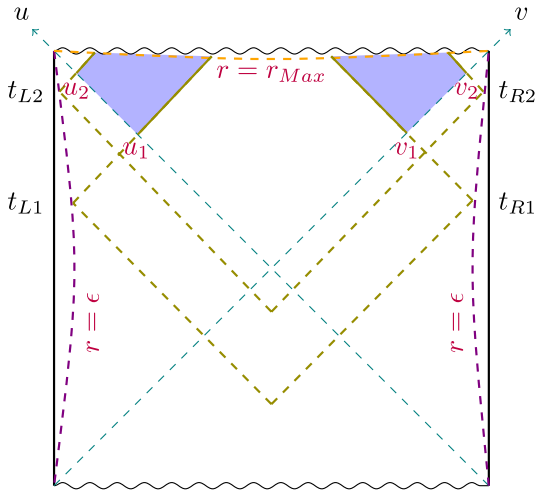

FIG. 3. Spacetime region corresponding to evaluation of holographic uncomplexity. The regions shown by the blue color compute uncomplexity given by Eq. (2.44). This is not equal to the difference between maximum complexity and the complexity of the state at a given time [see Eq. (2.46)].

Clearly, the on-shell action on the region depicted in Fig. 3 is given by a difference of the on-shell action evaluated on the future interior

$$I_{\rm UC} = I_{\rm FI\,2} - I_{\rm FI\,1} = 2M(\tau_2 - \tau_1), \tag{2.44}$$

where τ is the actual boundary time. It is also important to note that τ_2 should be thought of as a time cutoff, and eventually we are interested in the $\tau_2 \to \infty$ limit for some fixed τ_1. Indeed, the time cutoff could be set to $\tau_2 \sim \frac{\beta}{2\pi} e^{S_{\rm th}}$.

As we mentioned, the holographic uncomplexity is defined as the difference between maximum complexity and the complexity of the state at a given time; it is then evident from (2.44) that this equation cannot capture this difference. The crucial point is that the complexity, as we already mentioned, has two components: one from the boundary term and one from the joint point. The resultant uncomplexity given in Eq. (2.44) does not fully contain the contribution of joint point. To be precise, using Eq. (2.13), one has

$$\begin{aligned}\Delta I_{\rm WDW} &= I_2^{\rm WDW} - I_1^{\rm WDW} \\ &= \frac{V_d L^d}{8\pi G_N}\left[\frac{d-1}{2r_h^{d+1}}(\tau_2 - \tau_1) - \frac{\log|f(r_{m2})|}{r_{m2}^d} + \frac{\log|f(r_{m1})|}{r_{m1}^d}\right].\end{aligned} \tag{2.45}$$

One observes that there is a joint contribution that the subregion shown in Fig. 3 cannot see it, and thus it is not equal to $I_{\rm UC}$. Of course, it approaches $I_{\rm UC}$ when both r_{m1} and r_{m2} approach the horizon. Actually, using the fact that τ_2 should be thought of as a cutoff and therefore it is large (i.e., $r_{m2} \to r_h$), the above expression reads

$$\begin{aligned}\Delta I_{\rm WDW} \approx{}& 2M(\tau_2 - \tau_1) \\ &- \frac{V_d L^d}{8\pi G_N}\left[\frac{c_0}{r_h^d} - \frac{(d+1)\tau_1}{2r_h^{d+1}} - \frac{\log|f(r_{m1})|}{r_{m1}^d}\right].\end{aligned} \tag{2.46}$$

Note that the second part is just the on-shell action evaluated on the past interior that vanishes as r_{m1} approaches the horizon. It is worth mentioning that, although it is not clear from this expression, setting $\tau_1 = \tau_2$ the above equation vanishes. To see this, we note that in this expression the time τ_2 is associated with the limit where $r_{m2} \approx r_h$. Therefore, setting $\tau_1 = \tau_2$, the joint point r_{m1} approaches the horizon, too, and thus the expression in the bracket vanishes in this limit as well.

III. SUBREGION COMPLEXITY AND OUTSIDE THE HORIZON

In the previous section, we computed the on-shell action on different regions containing a part that is located behind the horizon. These regions could be found by the intersection of a WDW patch with the interior of a two-sided black brane. We have seen that the resultant on-shell action is time dependent whenever it receives a contribution from a region inside the black brane.

On the other hand, one may consider cases in which the subregions of interest are entirely outside the horizon. This is, indeed, what we would like to consider in this section. In this case, unlike in the previous cases, one usually gets time-independent on-shell action. In some cases, the region of interest could be thought of as the intersection of the WDW patch with the entanglement wedge.

A. Complexity of layered stretched horizon

Let us consider a subregion in the black hole exterior in the shape of a triangle shown in the left panel of Fig. 4. The three faces of the corresponding triangle are given by two null boundaries and a timelike boundary:

$$t = t_1 + r^*(\epsilon) - r^*(r), \quad t = t_2 - r^*(\epsilon) + r^*(r), \quad r = \epsilon. \tag{3.1}$$

The null boundaries intersect at the point $r = r_p$ that is given by

$$\tilde{\tau} \equiv t_{R2} - t_{R1} = 2(r^*(\epsilon) - r^*(r_p)), \tag{3.2}$$

where $\tilde{\tau}$ is the time interval. This should not be confused with the actual field theory time coordinate τ we have used in the previous section.

Actually following Ref. [1], in which the author considers a layered stretched horizon, this might be thought of as a bulk operator P localized at point r_p. Indeed, the corresponding triangle shows a region of the boundary

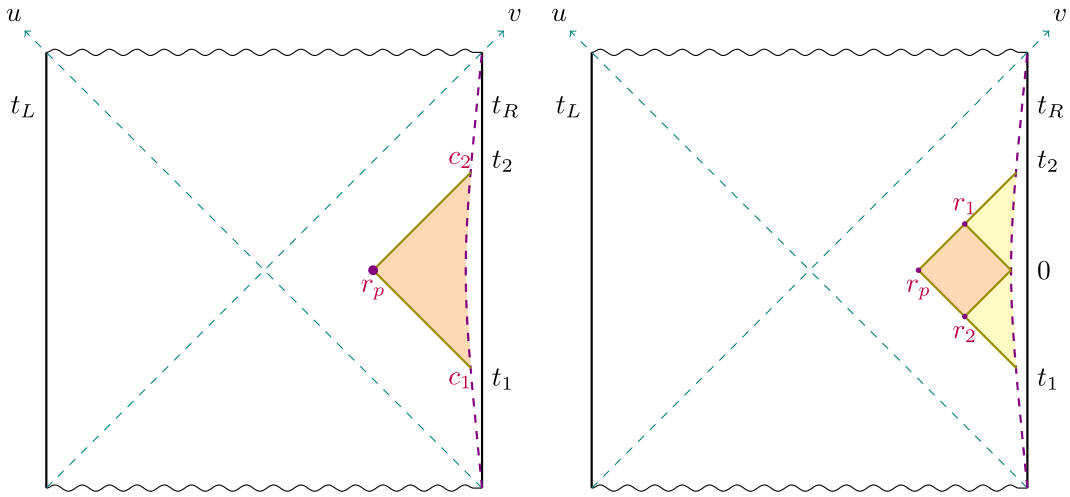

FIG. 4. *Left:* A localized operator at P. The colored region is the part that is involved in the construction of the operator localized at $r = r_p$. *Right:* The orange region is the intersection of the WDW patch and entanglement wedge at time slice $t_R = 0$ for half of an eternal black hole.

involved in the construction of the operator P. Now, the aim is to compute the on-shell action in this subregion. Following Ref. [1], the result might be thought of as complexity of the operator localized on the corresponding layer.

To proceed, let us start with the bulk contribution. From the notation depicted in Fig. 4, it is straightforward to see

$$I_{\text{Tri}}^{\text{bulk}} = -\frac{V_d L^d}{8\pi G_N}(d+1)\int_{\epsilon}^{r_p}\frac{dr}{r^{d+2}}(\tilde{\tau} - 2(r^*(\epsilon) - r^*(r))) = -\frac{V_d L^d}{8\pi G_N}\left(\frac{1}{\epsilon^{d+1}} - \frac{1}{r_h^{d+1}}\right)\tilde{\tau} + \frac{V_d L^d}{4\pi G_N d}\left(\frac{1}{\epsilon^d} - \frac{1}{r_p^d}\right). \tag{3.3}$$

As for the boundary terms, we only need to consider the Gibbons-Hawking-York term at the timelike boundary $r = \epsilon$,

$$I_{\text{Tri}}^{\text{surface}} = \frac{1}{8\pi G_N}\int d^d x \int_{t_1 + r^*(\epsilon) - r^*(r)}^{t_2 - r^*(\epsilon) + r^*(r)} dt\sqrt{h}K_t|_{r=\epsilon} = \frac{(d+1)V_d L^d}{8\pi G_N}\left(\frac{1}{\epsilon^{d+1}} - \frac{1}{2r_h^{d+1}}\right)\tilde{\tau}. \tag{3.4}$$

The normal vectors associated with the boundaries of the triangle given by (3.1) are

$$n_t = \frac{L dr}{\epsilon\sqrt{f(\epsilon)}}, \qquad k_1 = \alpha\left(-dt + \frac{dr}{f(r)}\right), \qquad k_2 = \beta\left(dt + \frac{dr}{f(r)}\right), \tag{3.5}$$

which can be used to compute the contribution of the joint points as follows:

$$\begin{aligned} I_{\text{Tri}}^{\text{joint}} &= \frac{1}{8\pi G_N}\int_{c_1} d^d x\sqrt{\gamma}\log|k_2\cdot n_t| + \frac{1}{8\pi G_N}\int_{c_2} d^d x\sqrt{\gamma}\log|k_1\cdot n_t| - \frac{1}{8\pi G_N}\int_{r_p} d^d x\sqrt{\gamma}\log\left|\frac{k_1\cdot k_2}{2}\right| \\ &= \frac{V_d L^d}{8\pi G_N}\frac{\log\frac{\alpha\beta\epsilon^2}{L^2}}{\epsilon^d} - \frac{V_d L^d}{8\pi G_N}\left(\frac{\log\frac{\alpha\beta r_p^2}{L^2}}{r_p^d} - \frac{\log f(r_p)}{r_p^d}\right). \end{aligned} \tag{3.6}$$

The contribution of the term needed to remove the ambiguity is

$$\begin{aligned} I_{\text{Tri}}^{\text{amb}} &= \frac{1}{8\pi G_N}\int_{\text{null}} d\lambda d^d x\sqrt{\gamma}\Theta\log\frac{|\tilde{L}\Theta|}{d} \\ &= \frac{V_d L^d}{8\pi G_N}\left(\frac{\log\frac{\alpha\beta\tilde{L}^2 r_p^2}{L^4}}{r_p^d} + \frac{2}{dr_p^d}\right) - \frac{V_d L^d}{8\pi G_N}\left(\frac{\log\frac{\alpha\beta\tilde{L}^2\epsilon^2}{L^4}}{\epsilon^d} + \frac{2}{d\epsilon^d}\right). \end{aligned} \tag{3.7}$$

Therefore, taking all contributions into account, one arrives at

$$I_{\text{Tri}} = \frac{V_d L^d}{8\pi G_N}\left[\left(\frac{d}{\epsilon^{d+1}} - \frac{d-1}{2r_h^{d+1}}\right)\tilde{\tau} + \left(\frac{1}{r_p^d} - \frac{1}{\epsilon^d}\right)\log\frac{\tilde{L}^2}{L^2} + \frac{\log f(r_p)}{r_p^d}\right]. \tag{3.8}$$

At this stage, we would like to recall that whenever one is dealing with the computation of on-shell action it is

important to make it clear what one means by action. As we already mentioned, by an action, we mean all terms needed to have a covariant action with a well-defined variational principle that result in a finite free energy. This, in particular, requires one to consider the counterterms that are obtained in the context of holographic renormalization. In the present case in which we have a timelike flat boundary at $r=\epsilon$, the corresponding counterterm is given by

$$I_{\rm Tri}^{\rm ct}=-\frac{1}{8\pi G_N}\int_{r=\epsilon}d^{d+1}x\sqrt{h}\frac{d}{L}, \tag{3.9}$$

which gives the following contribution to the on-shell action:

$$I_{\rm Tri}^{\rm ct}=\frac{V_dL^d}{8\pi G_N}\left(-\frac{d}{\epsilon^{d+1}}+\frac{d}{2r_h^{d+1}}\right)\tilde{\tau}. \tag{3.10}$$

Combining the above result with Eq. (3.8), the total on-shell action reads[10]

$$I_{\rm Tri}=\frac{V_dL^d}{8\pi G_N}\left[-\frac{1}{\epsilon^d}\log\frac{\tilde{L}^2}{L^2}+\frac{\tilde{\tau}}{2r_h^{d+1}}+\frac{\log\frac{\tilde{L}^2f(r_p)}{L^2}}{r_p^d}\right]. \tag{3.11}$$

Note that, since we have already assumed $\tilde{L}\geq L$, from the above expression, one finds that the most divergent term and the finite term are negative. This is, of course, in contrast to what one would expect from complexity. Actually, the result is reminiscent of free energy of the black hole. Indeed, denoting the contribution of joint point by $\mathcal{J}$, one has (dropping the divergent term)

$$I_{\rm Tri}=-\mathcal{F}\tilde{\tau}+\mathcal{J}_p\quad\text{with}\quad\mathcal{J}_p=\frac{\log f(r_p)}{r_p^d}, \tag{3.12}$$

where $\mathcal{F}=-\frac{V_dL^d}{16\pi G_N}\frac{1}{r_h^{d+1}}$ is the free energy of the corresponding black brane. To summarize, we note that the on-shell action in this case consists of two parts: the first part might be thought of as the classical contribution being the contribution of the timelike boundary that is the free energy of corresponding black brane, and the second one that comes from joint point should be treated as the new contribution associated with the complexity of the operator. Clearly, when a given subregion does not contain a timelike boundary, the free energy drops, and the whole contributions come from joint points (see the next subsection).

[10]We note that the resultant on-shell action is still divergent due to the ambiguity of fixing the length scale $\tilde{L}$. Of course, there is a natural way to fix this length scale by assuming that the corresponding on-shell action for an AdS geometry in the Poincaré coordinates vanishes (as a reference state), leading to $\tilde{L}=L$. Therefore, one ends up with a finite on-shell action.

For the case in which the point r_p is in the vicinity of the horizon, i.e., $r_p=r_h-\xi$ for $\xi\ll r_h$, from Eq. (3.11), one finds

$$I_{\rm Tri}\approx\frac{V_dL^d}{8\pi G_N}\left(\frac{1}{r_p^d}-\frac{1}{\epsilon^d}\right)\log\frac{\tilde{L}^2}{L^2}-\frac{V_dL^d}{16\pi G_N}\frac{1}{r_h^{d+1}}(d\tilde{\tau}), \tag{3.13}$$

which shows the layer (operator) becomes more complex as one approaches the horizon. In particular, when one is away from the horizon by about the Planck length, one gets

$$I_{\rm Tri}\approx\frac{V_dL^d}{8\pi G_N}\left(\frac{1}{r_p^d}-\frac{1}{\epsilon^d}\right)\log\frac{\tilde{L}^2}{L^2}-\frac{1}{2\pi(d+1)}S_{\rm th}\log S_{\rm th} \tag{3.14}$$

B. CA proposal and subregion complexity

An immediate application of the result we obtained in the previous section is to find on-shell action for a square subregion shown in orange in the right panel of Fig. 4. The result may be used to compute the on-shell action on a region obtained by the intersection of the entanglement wedge and WDW patch. The desired result can be found by algebraic summation of three triangles identified by r_1, r_2, and r_p. Actually, using Eq. (3.8), one gets[11]

$$\begin{aligned}I_{\rm Sq}&=I_{r_p}-I_{r_1}-I_{r_2}\\&=\frac{V_dL^d}{8\pi G_N}\left[\left(\frac{1}{\epsilon^d}+\frac{1}{r_p^d}-\frac{1}{r_1^d}-\frac{1}{r_2^d}\right)\log\frac{\tilde{L}^2}{L^2}\right.\\&\quad\left.+\frac{\log f(r_p)}{r_p^d}-\frac{\log f(r_1)}{r_1^d}-\frac{\log f(r_2)}{r_2^d}\right].\end{aligned} \tag{3.15}$$

Note that in this case the most divergent term is positive, as expected for an expression representing complexity. Indeed, since the corresponding subregion is the intersection of the WDW patch and domain of dependence of a subregion in the boundary theory (which is the whole system in the present case at time $\tau=0$), we would like to identify this expression as the CA subregion complexity [8]. Note that, since there are no timelike or spacelike boundaries, all contributions come from the joint points.

It is also interesting to consider the limit of $\{r_p,r_1,r_2\}\to r_h$, where we get a subregion shown in the left panel of Fig. 5. This is the intersection of the WDW patch at time slice $\tau=0$ with the right exterior of the black hole. Actually, by making use of Eq. (2.25) and with the notation shown in Fig. 5 in the limit of $\{r_p,r_1,r_2\}\to r_h$, Eq. (3.15) reads

[11]One could have directly computed the on-shell action for the square region, taking into account all terms in the action. Of course, the result is the same as what we have found by an algebraic summation of three triangles.

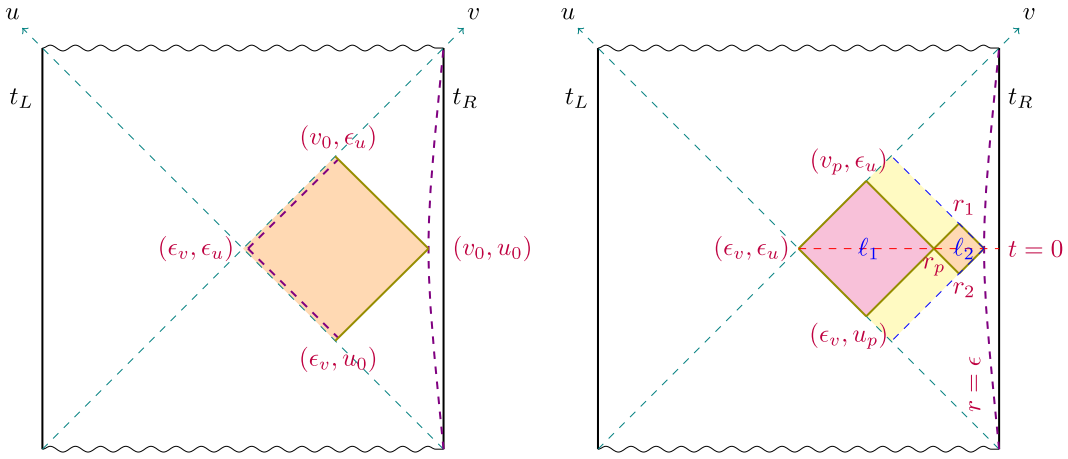

FIG. 5. *Left:* Intersection of the WDW patch and entanglement wedge for large entangling region at time slice $t_R = 0$ for half of an eternal black hole. *Right:* Two subregions denoted by ℓ_1 and ℓ_2.

$$I_{\rm Sq} = \frac{V_d L^d}{8\pi G_N}\left(\frac{1}{\epsilon^d} - \frac{1}{r_h^d}\right)\log\frac{\tilde{L}^2}{L^2} - \frac{c_0}{2\pi}S_{\rm th}. \tag{3.16}$$

It is important to note that, although the most divergent term is positive for $\tilde{L} > L$, the finite term is negative. We note that the on-shell action for the subregion shown in the left panel of Fig. 5 has been recently studied in Ref. [48], in which the authors do not consider the term needed to remove the ambiguity and fix the ambiguity by hand.[12] As a result, the finite term they find is positive. We note, however, that it is crucial to take into account the corresponding term to maintain the reparamerization invariance of the action. Note that for values of r_p it can be seen that the finite part of Eq. (3.15) is always negative.[13] It is also interesting to compare the on-shell action evaluated on different subregions and the union of the subregions. To proceed, we will consider two subregions denoted by ℓ_1 and ℓ_2 in the right panel of Fig. 5. Using the notation shown in the figure and setting $\tilde{L} = L$, one has

$$\begin{aligned} I_{\ell_1} &= \frac{V_d L^d}{8\pi G_N}\left(\frac{\log|f(r_p)|}{r_p^d} + \frac{\log|f(r_\epsilon)|}{r_h^d} - \frac{\log|f(r_{u_p})|}{r_h^d} - \frac{\log|f(r_{u_p})|}{r_h^d}\right) \\ &= \frac{V_d L^d}{8\pi G_N}\left(\frac{\log|f(r_p)|}{r_p^d} - \frac{c_0 + \log|u_p v_p|}{r_h^d}\right) = \frac{V_d L^d}{8\pi G_N}\left(\frac{\log|f(r_p)|}{r_p^d} - \frac{c_0 - f'(r_h)r^*(r_p)}{r_h^d}\right), \\ I_{\ell_2} &= \frac{V_d L^d}{8\pi G_N}\left(\frac{\log|f(r_p)|}{r_p^d} - \frac{\log|f(r_1)|}{r_1^d} - \frac{\log|f(r_2)|}{r_2^d}\right). \end{aligned} \tag{3.17}$$

Here, in order to simplify I_{ℓ_1}, we have used (2.25). On the other hand, the on-shell action evaluated on $\ell_1 \cup \ell_2$ is (3.16)

$$I_{\ell_1 \cup \ell_2} = -\frac{V_d L^d}{8\pi G_N}\frac{c_0}{r_h^d}. \tag{3.18}$$

Therefore, one gets

$$A \equiv I_{\ell_1} + I_{\ell_2} - I_{\ell_1 \cup \ell_2} = \frac{V_d L^d}{8\pi G_N}\left(2\frac{\log|f(r_p)|}{r_p^d} - \frac{(d+1)r^*(r_p)}{r_h^{d+1}} - \frac{\log|f(r_1)|}{r_1^d} - \frac{\log|f(r_2)|}{r_2^d}\right). \tag{3.19}$$

[12]We note that the contribution of the term removing the ambiguity has been added to the published version of Ref. [48], in which a proper citation to the present paper is also given.

[13]We would like to thank B. Swingle for discussions on this point.

It is then important to determine the sign of A. To do so, one first observes that A vanishes at both $\{r_p, r_1, r_2\} \to r_h$ and $\{r_p, r_1, r_2\} \to 0$ limits. On the other hand, one can show that at $\{r_p, r_1, r_2\} \approx 0$ the function A approaches zero from above, leading to the fact that $A \geq 0$. This behavior may also be shown numerically. As a result, we conclude that the on-shell action we have evaluated for subregions in the exterior of the black brane obeys subadditivity condition

$$I_{\ell_1} + I_{\ell_2} \geq I_{\ell_1 \cup \ell_2}, \tag{3.20}$$

which is indeed in agreement with results of Ref. [48] (see also Ref. [52]). It is worth noting that in order to reach the above result the contribution of the corner term, $\log u_p v_p$, plays a crucial role.

IV. DISCUSSIONS AND CONCLUSIONS

In this paper, motivated by the "complexity equals action" proposal, we have evaluated the on-shell action on certain spacetime subregions enclosed by null boundaries that, of course, includes the WDW patch itself, too. Our main concern was to compute finite term of the on-shell action. It is contrary to most studies in the literature, in which the main concern is to compute the growth rate of the complexity (see, e.g., Refs. [53–66]).

Although we have computed the on-shell action on a given subregion, taking into account all terms needed to have reparametrization invariance and well-defined variational principle, we have observed that the final result is given by contributions of joint points and timelike or spacelike boundaries. Removing the most divergent term by setting $\tilde{L} = L$, the corresponding joint contribution, $\mathcal{J}$, and timelike and spacelike surface contributions, $\mathcal{S}_t$, and $\mathcal{S}_s$, are given by

$$\mathcal{J} = \frac{V_d L^d}{8\pi G_N} \frac{\log|f(r)|}{r^d}, \qquad \mathcal{S}_t = \frac{V_d L^d}{8\pi G_N} \frac{\tilde{\tau}}{2r_h^{d+1}},$$
$$\mathcal{S}_s = \frac{V_d L^d}{8\pi G_N} \frac{(d-1)\tau}{2r_h^{d+1}}. \tag{4.1}$$

Note that when the joint point occurs at the horizon one needs to take the $r \to r_h$ limit from the above joint contribution $\mathcal{J}$ that typically results in an expression proportional to $\log|uv| + c_0$.

Clearly, when the joint point is located at the horizon, one needs to regularize the joint contribution using Eq. (2.25). The sign of the joint contribution depends on the position of the corresponding joint point. If the joint point is located on the left or right of the given subregion, the sign is positive, and for those that are located above or below the subregion, it is negative. It is also interesting to compute the time derivative of the above expressions,

$$\dot{\mathcal{J}} = \frac{V_d L^d}{8\pi G_N} \left(\frac{d+1}{2r_h^{d+1}} + \frac{d}{2r^d} f(r) \log|f(r)| \right),$$
$$\dot{\mathcal{S}}_t = 0, \qquad \dot{\mathcal{S}}_s = \frac{V_d L^d}{8\pi G_N} \frac{(d-1)}{2r_h^{d+1}}, \tag{4.2}$$

showing that in the late time the joint point has a nontrivial contribution.

Another observation we have made is that whenever the subregion contains a part of the black hole interior the finite part of the action is positive and time dependent, while for the cases in which the desired subregion is entirely in the exterior part of the black hole, the corresponding finite term is time independent and negative. It is also important to note that for all cases, except one, the most divergent term exhibits volume law scaling with a positive sign. These points should be taken into account when it comes to interpreting the results from a field theory point of view.

Throughout this paper, we have been careful enough to clarify what we mean by the on-shell action. Indeed, there are several terms one may add to the action that could alter the results once we compute the on-shell action. It is then important to fix them. Our physical constraints were to have reparametrization invariance and a well-defined variational principle. These assumptions enforce us to have certain boundary and joint actions. In particular, it was crucial to consider the log term given by Eq. (1.2) that is needed to remove the ambiguity associated with the null vectors. Actually, in our computations, this term has played an essential role.

We note, however, that, even with this term, the resultant on-shell action still contains an arbitrary length scale. We have chosen the length scale so that the most divergent term of the on-shell action is positive. This is indeed required if one wants to identify the on-shell action with complexity, at least when evaluated inside the WDW patch. Of course, following the general idea of the holographic renormalization, one may add certain counterterms to remove all divergent terms including that associated with the undetermined length scale [45]. This is, actually, what we have done in this paper when we were only interested in the finite part of the on-shell action.

In fact, if one wants to identify the on-shell action with the complexity, we may not be surprised to have an arbitrary length scale. This might be related to choosing an arbitrary length scale in the definition of complexity in quantum field theory (see, e.g., Refs. [22,23]). Of course, eventually, we would like to find a way to fix the length scale or at least to make a constraint on it so that it could naturally lead to a clear interpretation in terms of complexity.

The main question that remains to be addressed is how to interpret our results from a field theory point of view. It is well accepted that the on-shell action evaluated in the

WDW patch is associated with the computational complexity that is the minimum number of gates one needs to reach the desired target state from the reference state (usually the vacuum state). Of course, this is the complexity defined for a pure state. It is then natural to look for a definition of complexity for a mixed state. This has been partially addressed in Refs. [48,52].

Considering a pure state and focusing on an specific subsystem which is a mixed state and described by a reduced density matrix, it may be useful to define complexity for mixed states. Of course, the resultant subregion complexity could as well depend on the state of whole system whether or not it is pure.

Actually, different possible definitions of subregion complexity have been explored in Ref. [48]. Based on the results we have found, it seems that the on-shell action evaluated on a subregion in the exterior of the black hole is consistent with purification complexity [48]. The main observation supporting this proposal is the subadditivity condition satisfied by the corresponding on-shell actions.[14] Note that this is not the case for complexity obtained by complexity equals volume proposal.

Since we have been dealing with complexity for subregions, motivated by entanglement entropy and mutual information, it might be useful to define a new quantity associated with two subregions A and B as

$$\mathcal{C}(A|B) = \mathcal{C}(A) + \mathcal{C}(B) - \mathcal{C}(A \cup B), \tag{4.3}$$

which could be thought of as mutual complexity. Here, $\mathcal{C}$ stands for complexity evaluated using the CA proposal. It is also clear that the above expression is finite and symmetric under the exchange of A and B.

This quantity might be thought of as a quantum measure that measures the correlation between two subsystems. Of course, we should admit that the precise interpretation of this quantity is not clear to us. Nonetheless, it might be possible to explore certain properties of the quantity. In particular, it is interesting to determine the sign of the mutual complexity, which in turn could tell us whether the complexity is superadditive or subadditive.

Actually, with the context in which we have been studying the complexity in this paper, it is clear that if one considers two subregions from two different boundaries of the eternal black brane (one from the left boundaries and the other from the right boundaries) the above quantity is negative. More precisely, in this case, the mutual complexity is given in terms of the on-shell action evaluated in the past and future interiors multiplied by a minus sign (see, e.g., Sec. II. C. 2). Of course, note that in this case, since we have to consider all regions inside the horizon, the final results are time dependent.

On the other hand, if we are interested in the time-independent complexity, we will have to consider cases in which both regions are located at the same boundary of the eternal black brane as shown in the Penrose diagram in Fig. 5. In these cases, where the complexity is time independent, we will consider a time slice at $\tau = 0$. To explore the possible sign of the mutual complexity, we first note that in general there is an arbitrary length scale, i.e., $\tilde{L}$, in the expression of the complexity that could change the sign as one chooses different scales. This scale appears due to the ambiguity of the normalization of the null vectors [see Eq. (1.2)].

In fact, in Sec. III. B, we have shown that under the assumption of $\tilde{L} = L$ the subregion complexity is subadditive, which means the mutual complexity is positive. This is also consistent with the numerical result found in Ref. [52]. It is, however, important to note that *a priori* there is no reason to fix the new scale $\tilde{L}$ equal to L, which is the AdS radius.

Actually, it is straightforward to see that the sign of the mutual complexity defined above also depends on the ratio $\frac{\tilde{L}}{L}$. More precisely, from Eq. (3.15), one observes that there are terms proportional to $\log\frac{\tilde{L}^2}{L^2}$ that could contribute to the mutual complexity of which the value is negative for $\frac{\tilde{L}}{L} > 1$. Thus, this makes the mutual complexity negative. On the other hand, for $\frac{\tilde{L}}{L} \leq 1$, their contributions are positive, which in turn makes the mutual complexity positive, too.

To conclude, we note that the mutual complexity is positive for the cases in which the subregion complexity is time independent and moreover $\frac{\tilde{L}}{L} \leq 1$. It would be interesting to further explore properties of the mutual complexity that could be thought of as a quantity that diagnoses whether the complexity is sub- or superadditive.

ACKNOWLEDGMENTS

The authors would like to kindly thank A. Akhavan, J. L. F. Barbon, A. Naseh, F. Omidi, B. Swingle, M. R. Tanhayi, and M. H. Vahidinia for useful comments and discussions on related topics. We would also like to thank the referee for his/her useful comment.

[14]We would like to thank B. Swingle for discussions on this point.

[1] L. Susskind, Computational complexity and black hole horizons, Fortschr. Phys. **64**, 24 (2016).

[2] D. Stanford and L. Susskind, Complexity and shock wave geometries, Phys. Rev. D **90**, 126007 (2014).

[3] A. R. Brown, D. A. Roberts, L. Susskind, B. Swingle, and Y. Zhao, Holographic Complexity Equals Bulk Action, Phys. Rev. Lett. **116**, 191301 (2016).

[4] A. R. Brown, D. A. Roberts, L. Susskind, B. Swingle, and Y. Zhao, Complexity, action, and black holes, Phys. Rev. D **93**, 086006 (2016).

[5] M. Alishahiha, Holographic complexity, Phys. Rev. D **92**, 126009 (2015).

[6] O. Ben-Ami and D. Carmi, On volumes of subregions in holography and complexity, J. High Energy Phys. 11 (2016) 129.

[7] J. Couch, W. Fischler, and P. H. Nguyen, Noether charge, black hole volume and complexity, J. High Energy Phys. 03 (2017) 119.

[8] D. Carmi, R. C. Myers, and P. Rath, Comments on Holographic Complexity, J. High Energy Phys. 03 (2017) 118.

[9] R. Abt, J. Erdmenger, H. Hinrichsen, C. M. Melby-Thompson, R. Meyer, C. Northe, and I. A. Reyes, Topological complexity in AdS_3/CFT_2, Fortschr. Phys. **66**, 1800034 (2018).

[10] R. Abt, J. Erdmenger, M. Gerbershagen, C. M. Melby-Thompson, and C. Northe, Holographic subregion complexity from kinematic space, J. High Energy Phys. 01 (2019) 012.

[11] E. Bakhshaei, A. Mollabashi, and A. Shirzad, Holographic subregion complexity for singular surfaces, Eur. Phys. J. C **77**, 665 (2017).

[12] B. Chen, W. M. Li, R. Q. Yang, C. Y. Zhang, and S. J. Zhang, Holographic subregion complexity under a thermal quench, J. High Energy Phys. 07 (2018) 034.

[13] D. S. Ageev, I. Y. Aref'eva, A. A. Bagrov, and M. I. Katsnelson, Holographic local quench and effective complexity, J. High Energy Phys. 08 (2018) 071.

[14] M. Miyaji, T. Takayanagi, and K. Watanabe, From path integrals to tensor networks for the AdS/CFT correspondence, Phys. Rev. D **95**, 066004 (2017).

[15] P. Caputa, N. Kundu, M. Miyaji, T. Takayanagi, and K. Watanabe, Anti-de Sitter Space from Optimization of Path Integrals in Conformal Field Theories, Phys. Rev. Lett. **119**, 071602 (2017).

[16] P. Caputa, N. Kundu, M. Miyaji, T. Takayanagi, and K. Watanabe, Liouville action as path-integral complexity: From continuous tensor networks to AdS/CFT, J. High Energy Phys. 11 (2017) 097.

[17] T. Takayanagi, Holographic spacetimes as quantum circuits of path-integrations, J. High Energy Phys. 12 (2018) 048.

[18] D. Carmi, S. Chapman, H. Marrochio, R. C. Myers, and S. Sugishita, On the time dependence of holographic complexity, J. High Energy Phys. 11 (2017) 188.

[19] S. Lloyd, Ultimate physical limits to computation, Nature (London) **406**, 1047 (2000).

[20] M. Moosa, Evolution of complexity following a global quench, J. High Energy Phys. 03 (2018) 031.

[21] K. Hashimoto, N. Iizuka, and S. Sugishita, Time evolution of complexity in Abelian gauge theories, Phys. Rev. D **96**, 126001 (2017).

[22] R. Jefferson and R. C. Myers, Circuit complexity in quantum field theory, J. High Energy Phys. 10 (2017) 107.

[23] S. Chapman, M. P. Heller, H. Marrochio, and F. Pastawski, Toward a Definition of Complexity for Quantum Field Theory States, Phys. Rev. Lett. **120**, 121602 (2018).

[24] R. Q. Yang, Complexity for quantum field theory states and applications to thermofield double states, Phys. Rev. D **97**, 066004 (2018).

[25] R. Khan, C. Krishnan, and S. Sharma, Circuit complexity in Fermionic field theory, Phys. Rev. D **98**, 126001 (2018).

[26] R. Q. Yang, Y. S. An, C. Niu, C. Y. Zhang, and K. Y. Kim, Principles and symmetries of complexity in quantum field theory, Eur. Phys. J. C **79**, 109 (2019).

[27] L. Hackl and R. C. Myers, Circuit complexity for free fermions, J. High Energy Phys. 07 (2018) 139.

[28] D. W. F. Alves and G. Camilo, Evolution of complexity following a quantum quench in free field theory, J. High Energy Phys. 06 (2018) 029.

[29] A. Bhattacharyya, P. Caputa, S. R. Das, N. Kundu, M. Miyaji, and T. Takayanagi, Path-integral complexity for perturbed CFTs, J. High Energy Phys. 07 (2018) 086.

[30] M. Guo, J. Hernandez, R. C. Myers, and S. M. Ruan, Circuit complexity for coherent states, J. High Energy Phys. 10 (2018) 011.

[31] A. Bhattacharyya, A. Shekar, and A. Sinha, Circuit complexity in interacting QFTs and RG flows, J. High Energy Phys. 10 (2018) 140.

[32] R. Q. Yang, Y. S. An, C. Niu, C. Y. Zhang, and K. Y. Kim, More on complexity of operators in quantum field theory, J. High Energy Phys. 03 (2019) 161.

[33] R. Q. Yang, C. Niu, C. Y. Zhang, and K. Y. Kim, Comparison of holographic and field theoretic complexities for time dependent thermofield double states, J. High Energy Phys. 02 (2018) 082.

[34] M. Moosa, Divergences in the rate of complexification, Phys. Rev. D **97**, 106016 (2018).

[35] B. Swingle and Y. Wang, Holographic complexity of Einstein-Maxwell-Dilaton gravity, J. High Energy Phys. 09 (2018) 106.

[36] J. W. York, Jr., Role of Conformal Three Geometry in the Dynamics of Gravitation, Phys. Rev. Lett. **28**, 1082 (1972).

[37] G. W. Gibbons and S. W. Hawking, Action integrals and partition functions in quantum gravity, Phys. Rev. D **15**, 2752 (1977).

[38] K. Parattu, S. Chakraborty, B. R. Majhi, and T. Padmanabhan, A boundary term for the gravitational action with null boundaries, Gen. Relativ. Gravit. **48**, 94 (2016).

[39] L. Lehner, R. C. Myers, E. Poisson, and R. D. Sorkin, Gravitational action with null boundaries, Phys. Rev. D **94**, 084046 (2016).

[40] A. Reynolds and S. F. Ross, Divergences in holographic complexity, Classical Quantum Gravity **34**, 105004 (2017).

[41] M. Alishahiha, A. F. Astaneh, M. R. M. Mozaffar, and A. Mollabashi, Complexity growth with Lifshitz scaling and hyperscaling violation, J. High Energy Phys. 07 (2018) 042.

[42] S. Chapman, H. Marrochio, and R. C. Myers, Holographic complexity in Vaidya spacetimes. Part I, J. High Energy Phys. 06 (2018) 046.

[43] S. Chapman, H. Marrochio, and R. C. Myers, Holographic complexity in Vaidya spacetimes. Part II, J. High Energy Phys. 06 (2018) 114.
[44] K. Skenderis, Lecture notes on holographic renormalization, Classical Quantum Gravity **19**, 5849 (2002).
[45] A. Akhavan and F. Omidi, Complexity and the role of counter terms (to appear).
[46] S. Chapman, H. Marrochio, and R. C. Myers, Complexity of formation in holography, J. High Energy Phys. 01 (2017) 062.
[47] J. L. F. Barbon and J. Martin-Garcia, Terminal holographic complexity, J. High Energy Phys. 06 (2018) 132.
[48] C. A. Agon, M. Headrick, and B. Swingle, Subsystem complexity and holography, J. High Energy Phys. 02 (2019) 145.
[49] A. R. Brown and L. Susskind, Second law of quantum complexity, Phys. Rev. D **97**, 086015 (2018).
[50] Y. Zhao, Uncomplexity and black hole geometry, Phys. Rev. D **97**, 126007 (2018).
[51] H. Stoltenberg, Properties of the (Un)complexity of subsystems, Phys. Rev. D **98**, 126012 (2018).
[52] H. A. Camargo, P. Caputa, D. Das, M. P. Heller, and R. Jefferson, Complexity as a Novel Probe of Quantum Quenches: Universal Scalings and Purifications, Phys. Rev. Lett. **122**, 081601 (2019).
[53] D. Momeni, M. Faizal, S. Bahamonde, and R. Myrzakulov, Holographic complexity for time-dependent backgrounds, Phys. Lett. B **762**, 276 (2016).
[54] M. Alishahiha, A. F. Astaneh, A. Naseh, and M. H. Vahidinia, On complexity for F(R) and critical gravity, J. High Energy Phys. 05 (2017) 009.
[55] K. Nagasaki, Complexity of AdS_5 black holes with a rotating string, Phys. Rev. D **96**, 126018 (2017).
[56] Y. G. Miao and L. Zhao, Complexity-action duality of the shock wave geometry in a massive gravity theory, Phys. Rev. D **97**, 024035 (2018).
[57] M. Ghodrati, Complexity growth in massive gravity theories, the effects of chirality, and more, Phys. Rev. D **96**, 106020 (2017).
[58] M. M. Qaemmaqami, Complexity growth in minimal massive 3D gravity, Phys. Rev. D **97**, 026006 (2018).
[59] L. Sebastiani, L. Vanzo, and S. Zerbini, Action growth for black holes in modified gravity, Phys. Rev. D **97**, 044009 (2018).
[60] P. A. Cano, R. A. Hennigar, and H. Marrochio, Complexity Growth Rate in Lovelock Gravity, Phys. Rev. Lett. **121**, 121602 (2018).
[61] Y. S. An, R. G. Cai, and Y. Peng, Time dependence of holographic complexity in Gauss-Bonnet gravity, Phys. Rev. D **98**, 106013 (2018).
[62] R. Fareghbal and P. Karimi, Complexity growth in flat spacetimes, Phys. Rev. D **98**, 046003 (2018).
[63] M. Ghodrati, Complexity growth rate during phase transitions, Phys. Rev. D **98**, 106011 (2018).
[64] S. J. Zhang, Subregion complexity and confinement-deconfinement transition in a holographic QCD model, Nucl. Phys. **B938**, 154 (2019).
[65] S. Mahapatra and P. Roy, On the time dependence of holographic complexity in a dynamical Einstein-dilaton model, J. High Energy Phys. 11 (2018) 138.
[66] M. R. Tanhayi, R. Vazirian, and S. Khoeini-Moghaddam, Complexity growth following multiple shocks, Phys. Lett. B **790**, 49 (2019).